

# Reconfigurable RF multiband filter with widely tunable passbands based on cascaded optical interferometric filters

Jia Ge, *Student Member, IEEE*, and Mable P. Fok, *Member, IEEE*

**Abstract**— Despite the increasing importance and critical needs, reconfigurable radio frequency (RF) multiband filters are currently underdeveloped even both RF electronics and photonics technologies are being explored. Although RF multiband filters with large numbers of simultaneous passbands and wide frequency tuning range are extremely desired, achieving such functionality is extremely challenging. In this paper, a photonics based highly tunable and reconfigurable RF multiband filter is proposed through the combination of a special designed tunable Mach-Zehnder interferometer and a reconfigurable Lyot loop filter. Both the passband frequencies and the number of simultaneous passbands are adjustable, that one or multiple passbands are continuously tuned over a 20 GHz frequency range, and the number of simultaneous passbands are reconfigurable from zero to seven. As a result, the proposed RF multiband filter can be configured with various passband combinations through the same setup, providing exceptional operation flexibility. Furthermore, broadband operation and excellent filter selectivity is obtained, with sharp passband profiles and over 35 dB sidelobe suppression.

**Index Terms**— Microwave Photonics, Multiband Filter, Reconfigurable RF Filter, Tunable Filter, FIR filter.

## I. INTRODUCTION

Due to the ever-increasing demand of multiband wireless and satellite systems, multi-service systems and multi-function devices, multiband communications are of critical need in various radio frequency (RF) systems [1-3]. Multiband communications and frequency multiplexing are extremely useful to improve system spectral efficiency, multi-function capability, and heterogeneous types of services, where several frequency channels over a wide RF range are implemented simultaneously in the same system or same device. Thus, an RF bandpass filter with multiple passbands and high reconfigurability and tunability is a critical component [4] for channel selection and preventing interference. Although the need is clear, achieving such functionality is very challenging

This work was supported in part by the National Science Foundation (Award number: CMMI 1400100 and ECCS 1653525).

Jia Ge was with the Lightwave and Microwave Photonics Laboratory, College of Engineering, The University of Georgia, Athens, GA 30602, USA (e-mail: [jiage@uga.edu](mailto:jiage@uga.edu)).

Mable P. Fok was with the Lightwave and Microwave Photonics Laboratory, College of Engineering, The University of Georgia, Athens, GA 30602, USA (e-mail: [mfok@uga.edu](mailto:mfok@uga.edu)).

due to the nature of conventional electronic techniques --- lack of operation flexibility. Furthermore, it is challenging to satisfy the design parameters for all passbands when a large number of simultaneous passbands is required, which would result in non-uniform and inconsistent merits of different passbands [5]. For state-of-the-art electronics based RF multiband filters, the maximum number of simultaneous passbands achieved is six with fixed passband frequencies [6]; and very few tunable tri-band and quad-band filters have been realized with limited tuning range [4,7]. Although electronic approaches offer chip-size solutions, both the number of simultaneous passbands and passband tunability are extremely limited [4]. A promising way to implement RF multiband filters with high passband reconfigurability and frequency tuning capability is urgently desired.

Photonic technology has attracted considerable attention to achieve unique RF functions and enhance conventional RF systems, due to its unique properties such as wide operation bandwidth, excellent tunability, and reconfigurability [8-12]. Among these, tunable microwave photonic (MWP) single bandpass filter is always an active research topic and different approaches have been reported [13-24]. While highly tunable single passband filters have been well developed, however, despite the fact that RF multiband filter is also of critical needs, MWP multiband filters are still underdeveloped. Recently, the increasing number of MWP multiband filter demonstrated not just show the great interest of achieving multiband filters, they also reveal the practical challenges that MWP multiband filters is facing – it is hard to obtain tunable/reconfigurable multiple passbands with desired spectral profiles using conventional MWP filter architectures. A MWP multiband filter with three switchable passbands has been achieved using three pieces of birefringence fibers [25], and several tunable MWP dual-band filter approaches have also been explored [26-29]. A big step is taken forward through the use of a two-stage Lyot loop filter [30], that a passband switchable MWP multiband filter with up to twelve simultaneous passbands has been demonstrated. However, the resultant passbands can only be configured within the 12 specific pre-designed frequency channels. Fiber length will have to be changed to modify the preset frequency channel, which is impractical in real applications. To fulfill the functionality and flexibility needed in dynamic multiband systems, continuously tuning of some/all of the passbands to match with the desired frequencies is highly desired and will significantly advance filtering capability.

In this paper, we present a broadband MWP multiband filter with continuous frequency tunable and reconfigurable passbands. The passband frequencies can be continuously tuned and cover a large frequency range without any blind-point, while the number of simultaneous passbands is also adjustable from zero to seven. The proposed scheme is based on the combination of a tunable Mach-Zehnder interferometer (MZI) and a reconfigurable Lyot loop filter to generate high-order optical comb with variable comb spacing and comb combination. Unlike other previously demonstrated approaches, the use of both MZI and Lyot loop filter provides both frequency tunability and passband reconfigurability. As a result, the MWP multiband filter can be operated in several states through the same system setup --- single-band state, all-block state, dual-band and various multiband states --- all with tunable and reconfigurable passbands. To the best of our knowledge, this is the first demonstration of a RF multiband filter with such a flexible operation capability and a large number of tunable passbands. Furthermore, the generation of high order optical comb filters provides a general methodology for implementing RF filters with large number of simultaneous passbands through MWP filter technique.

## II. SYSTEM SETUP AND OPERATION PRINCIPLE

Figure 1 shows the schematic diagram of the proposed MWP multiband filter based on finite impulse response (FIR) filter architecture, a finite set of delayed and weighted signal taps are combined to implement the desired filter response. The multiband filter consists of two interferometric optical filters: the tunable MZI brings the continuous tunability to the RF filter design and the Lyot loop filter provides the reconfigurability of the number of simultaneous passbands. A broadband source is used as the light source and reshaped by a 30-nm wide optical Gaussian filter. The reshaped broadband source is then spectrally sliced by a tunable MZI and a Lyot loop filter to generate optical frequency comb with variable comb spacings. The optical frequency comb works as a multi-wavelength optical carrier, which is then modulated by the RF input signal through an electro-optic phase modulator. The modulated optical comb, now is the multi-tap signal, is then launched into a dispersive medium for acquiring constant time

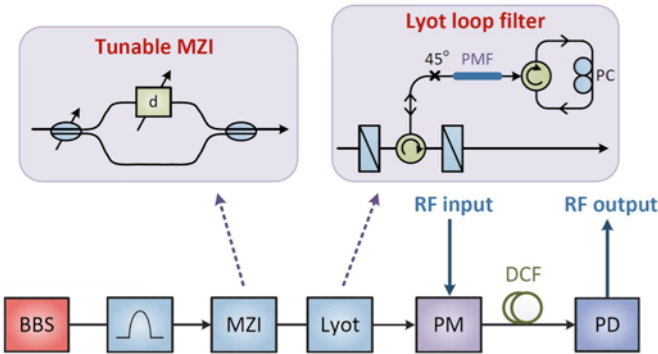


Fig. 1. Schematic diagram of the tunable and reconfigurable MWP multiband RF filter. BBS: broadband light source; MZI: Mach-Zehnder interferometer; d: tunable temporal delay line; PC: polarization controller; PM: phase modulator; DCF: dispersion compensating fiber; PMF: polarization maintaining fiber; PD: photo-detector.

delay difference between each of the filter taps. Each of the comb lines works as a single tap, which is temporally delayed by the DCF and previously weighted by the Gaussian optical filter to construct the desired MWP filter response. The weighted and delayed signal is then fed into a photo-detector and converted back to a RF signal at the output.

According to the principle of FIR filter, frequency response of the MWP filter can be expressed as the summation of a series of weighted and delayed copies of the RF input signal, as in Eq. (1),

$$H(\Omega) \propto \sum_{n=1}^N P_n \cdot e^{-j\Omega n T} \quad (1)$$

where  $\Omega$  is the microwave frequency,  $N$  is the total number of tap (number of comb lines) of the MWP filter,  $P_n$  is the power of the  $n^{\text{th}}$  tap of the optical comb, and  $T$  is the differential delay between each adjacent taps. A large tap number is desired to obtain a high Q factor in the RF filter, which is achieved by spectrally slicing a broadband light source (BBS) through optical comb filters. The comb spacings  $\Delta\omega$  of the MZI and Lyot loop filter determine the carrier wavelength spacing between each taps in the MWP multiband filter, which in turn governs the temporal delay  $T$  between taps as

$$T = \Delta\omega \cdot \beta_2 \cdot L_D \quad (2)$$

where  $\beta_2$  and  $L_D$  are the group velocity dispersion and length of the DCF, respectively. By apodizing the tap amplitudes with a broadband Gaussian optical filter, clean and sharp bandpass profile with high main-to-sidelobe suppression ratio (MSSR) can be resulted in the MWP filter. The passband center frequency ( $\Omega_0$ ) is determined by Eq. (3) [15-17].

$$\Omega_0 = \frac{2\pi}{\beta_2 L_D \Delta\omega} \quad (3)$$

For a system with a fixed dispersion, passband center frequency can be adjusted by varying the carrier frequency spacing of the filter taps, which in turn can be controlled by the comb spacing of the tunable optical comb filters ( $\Delta\omega$ ), i.e., the tunable MZI and Lyot Loop filter in the proposed setup. Furthermore, in order to simultaneously generate multiple passbands, multiple optical frequency combs with different comb spacings are required. This can be achieved by cascading multiple optical interferometric filters and generating high-order optical frequency combs [25,30]. The detailed operating principle of the tunable MZI and Lyot Loop filter will be discussed together with their performance in the next section.

$$\delta\Omega_{3\text{dB}} = \frac{\sqrt{8 \ln 2}}{\beta_2 L_D \delta\omega} \quad (4)$$

The 3-dB passband bandwidth is determined by Eq. (4) when the third-order dispersive term ( $\beta_3$ ) of the dispersion medium is neglected [15,17], where  $\delta\omega$  represents the overall bandwidth of the optical comb. As shown, the 3-dB bandwidth of the MWP filter is inversely proportional to the overall bandwidth of the optical comb, which can be pre-designed to fit the application needs. The dispersive medium used in the setup is a piece of 10.2-km DCF with a dispersion of -149.36 ps/(nm·km) (at 1530 nm) to provide time delays between each taps. A chirped fiber Bragg grating (CFBG) or photonic crystal waveguide with tunable delays can be used to replace the DCF for reducing the loss and size of the system [24, 32].

It is worth noticing that the carrier suppression effect (or dispersion-induced power fading effect) during the phase-modulation to intensity-modulation conversion process at the DCF would affect the amplitude uniformity of passbands at certain frequencies (i.e. below 2 GHz in particular). This phenomenon could be mitigated by replacing the phase modulator used for EO conversion by an intensity modulator. With an intensity modulator, additional passband at the baseband that corresponds to a low pass response will be present in the resultant RF filter [33].

### III. RESULTS AND DISCUSSION

#### A. MZI for enabling continuously passband frequency tuning in MWP filter

To better understand the principle of implementing both continuous frequency tunability and passband reconfigurability of the MWP multiband filter, we measured the performance and discussed the role of each section of the system as follow. We first investigate the role and performance of the tunable MZI and its corresponding role in the MWP filter by disabling the Lyot loop filter. As illustrated in the inset of Fig. 1, the tunable MZI is a modified two-branch interferometer, which consists of a tunable coupler at the input to adjust the power ratio between the two branches, and a tunable delay line to vary the path length difference  $d$  between the two branches. A standard 50:50 coupler is used to combine the two branches for interference. Based on the path difference  $d$  between the two branches, the two beams arrive at the coupler with a phase difference such that different extent of constructive interference or destructive interference is resulted at each wavelength ( $\lambda$ ). The phase difference between the two branches at each wavelength can be determined by Eq. (5),

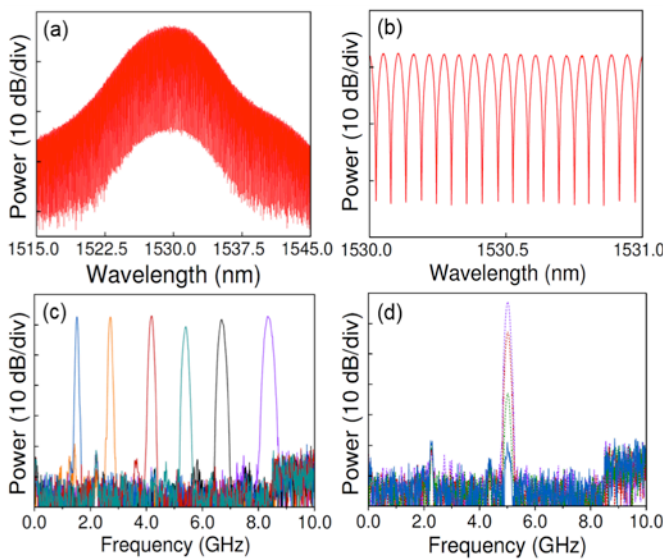


Fig. 2. Mach-Zehnder interferometer based MWP single bandpass filter with continuously tunability and reconfigurability. (a) Measured optical spectrum of the Gaussian profile optical frequency comb generated from the MZI. (b) Close-up of the optical comb in 1 nm range with a frequency spacing of 65 pm. (c) Measured frequency response of the RF single bandpass filter tuned to different frequencies. (d) The passband can be adjusted between ON/OFF states.

$$\varphi(\lambda) = \frac{2\pi n_e d}{\lambda} \quad (5)$$

and the corresponding comb spacing of the resultant optical comb filter is determined by Eq. (6),

$$\Delta\omega = \frac{2\pi c}{BL_e} \quad (6)$$

where  $n_e$  is the refractive index of the fiber used in the tunable MZI, and  $c$  is the speed of light. Figure 2(a) shows the measured optical spectrum of the broadband source that is reshaped by a Gaussian optical filter and spectrally sliced by the MZI. A close-up look of a 1 nm portion of the optical comb is shown in Fig. 2(b), showing a comb spacing of 65 pm. The corresponding RF response is shown in Fig. 2(c), where a single bandpass RF filter is observed and the center frequency is tunable over a wide frequency range by adjusting the comb spacing of the MZI through the tuning of  $d$  through the delay line. It is worth noticing that a wider passband bandwidths are observed at higher frequencies which is due to the slight differences in the dispersion slopes ( $\beta_3$ ) of the DCF over different wavelengths [15,17]. A tunable optical coupler with adjustable coupling ratio is used to vary the power ratio between the two MZI branches, such that the amplitude of the resultant passband is dynamically tunable over a 58 dB range, which essentially can go down to the noise floor -- switching off the channel, as shown in Fig. 2(d). Passband frequency tuning range of the single bandpass RF filter generated from the MZI is determined by the tuning range of the optical delay line. In the setup, a 17.5 ps time delay change will result in a 1 GHz tuning of the passband center frequency (shown in Fig. 4(b)), and the maximum tuning range is up to 35 GHz with the use of a 600 ps tunable delay line.

#### B. Lyot loop filter for reconfiguring the desired passbands in MWP filter

While the tunable MZI provides continuous tunability in passband frequency, passband reconfigurability is provided by the Lyot loop filter. As shown in Fig. 1, the Lyot loop filter [14] consists of a piece of polarization maintaining fiber (PMF), a polarization controller (PC), two aligned polarizers and two optical circulators. Since the PMF is a birefringent device, a phase difference of  $\Delta\varphi=2\pi BL/\lambda$  is obtained between the fast and slow axis when the light is aligned at 45° with respect to the fast axis, where  $B$  and  $L$  are the birefringence and length of the PMF, and  $\lambda$  is the wavelength of the light. By allowing the light to propagate twice in the PMF through the circulator-PC loop and adjusting the PC to have a variable polarization rotation angles ( $\Delta\theta$ ) of 0°, 45°, or 90°, a total phase difference ( $\sum\Delta\varphi$ ) of 2Δφ, Δφ and 0 can be obtained at the output, respectively. With different polarization rotation angles  $\Delta\theta$ , the equivalent length ( $L_e$ ) of the PMF is adjustable to 2L, L and 0, correspondingly, without physically changing the fiber length. As a result, an optical comb with switchable line spacings is achieved, and the comb spacing is determined by the equivalent length of PMF, as shown in Eq. (7).

$$\Delta\omega = \frac{2\pi c}{BL_e} \quad (7)$$

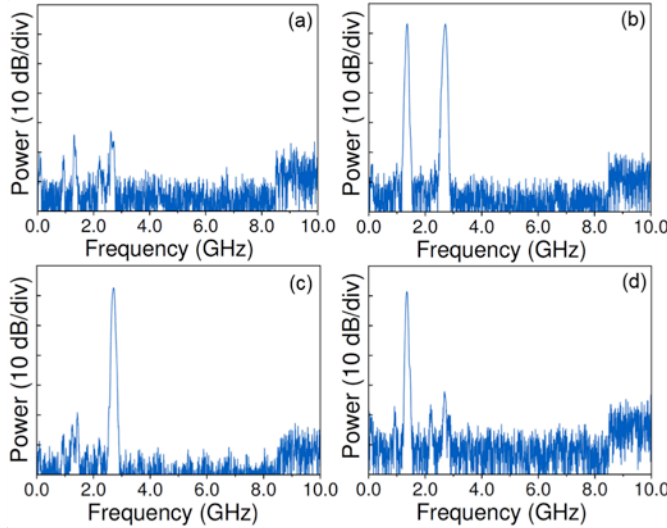


Fig. 3. Reconfigurable MWP dual-band filter based on Lyot loop filter. The RF filter is switched between four different operation states. (a) All-block state with no passband. (b) Dual-band state with two passbands at 1.35 GHz and 2.70 GHz. (c) Single-band state with a passband at 4.8 GHz. (d) Single-band state with a passband at 9.6 GHz.

The length of the PMF used in the setup is 12.15 m with a birefringence of  $6.33 \times 10^{-4}$ . The Lyot loop filter can be configured to have two interleaving combs by setting  $\Delta\theta$  to a value between  $0^\circ$  and  $45^\circ$ , such that the comb spacings generated from  $L$  and  $2L$  are obtained at the same time. Two optical combs are interleaving with each other, with different comb spacings of 304.2 pm and 152.1 pm. Consequently, two passbands are generated at the same time at 1.35 GHz and 2.70 GHz in the RF domain with MSSR over 40 dB, which is shown in Fig. 3(b). By adjusting the polarization rotation angles in the circulator-PC loop, different comb spacing combinations in the optical comb are achieved, and each of the passbands can be independently switched ON or OFF correspondingly. As a result, various operation states of the MWP filter can be configured, as shown in Fig. 3(a) to Fig. 3(d).

It is worth noticing that since the spectrally sliced optical frequency combs from both the MZI and Lyot Loop filter are sinusoidal and continuous sampled, the free spectral range (FSR) of the generated RF bandpass filter tends to infinity. As a result, only single-bandpass filter response is generated from each of the comb spacing ( $\Delta\omega$ ), instead of periodical passbands [15].

### C. Continuously tunable and reconfigurable MWP multiband filter based on cascaded MZI-Lyot architecture

The proposed RF multiband filter utilizes the MZI-Lyot architecture to enable continuous tunability, multiband capability, and high reconfigurability of the passbands. The MZI is a tunable first order comb filter, while the Lyot loop filter is a reconfigurable second-order comb filter, thus, by cascading the MZI and Lyot loop filter together, a reconfigurable high-order comb filter with multiple comb spacings can be achieved. Figure 4 shows the measured tuning results of the MWP multiband filter, seven passbands are generated at the same time and are marked as #1 to #7.

Passbands #1 and #2 are generated directly from Lyot loop filter, as shown in Fig. 3(b) in the previous section. Passband #5 is generated directly from the tunable MZI, while passbands #3, #4, #6 and #7 are generated by the addition and subtraction of the cascaded MZI and Lyot loop filter, as described by Table 1. As shown, passband #4 and #6 are generated from the interacting between the first passband from Lyot loop filter and MZI (Lyot1: #1 and MZI: #5), such that the frequency spacing between #4 (#6) and #5 is 1.35 GHz, which is explained as MZI-Lyot 1 and MZI + Lyot 1. Correspondingly, passband #3 and #7 are the cascading results of the second passband of Lyot loop filter and MZI (#2 and #5), which has a frequency spacing of 2.70 GHz away from passband #5 as MZI - Lyot 2 and MZI + Lyot 2.

The relationship between all seven passbands and their corresponding comb spacings generated from the cascaded MZI and Lyot loop filter are summarized in Table 1, where the seven passbands are set to be evenly distributed within a 10 GHz range, as indicated in Fig. 4(a). Since passband #5 is generated from a continuously tunable MZI, any passbands related to #5 are also continuously tunable, which are passbands #3, #4, #5, #6 and #7. Figure 4(c) to 4(e) show the measured tuning performance, the right five passbands (#3 to #7) generated from the MZI are continuously tuned over 20 GHz. The MSSR for all the passband are over 35 dB and the average 3-dB bandwidth is about 100 MHz, resulting a passband Q-factor of 200 at 20 GHz. The insertion loss is about 10-15 dB over different passbands, and can be improved by adding optical amplifiers after the PM. The frequency spacing between each passband among the five tunable passbands is kept the same intentionally, which is determined by the length of the PMF inside the Lyot loop filter. Figure 4(b) shows the relationship between the passband frequency and the path length difference between the two branches of the MZI. The maximum frequency tuning range is up to 35 GHz with the current setup, and is determined by the optical tunable delay line in MZI. The largest amplitude difference among all the seven passbands is less than 10 dB, which is mainly caused by the amplitude difference between the interleaved optical frequency combs for generating the passbands. Further amplitude compensation using optical amplifiers could improve the amplitude uniformity of the passbands.

Passbands reconfigurability of the proposed RF multiband filter is achieved by adjusting the polarization rotation angle  $\Delta\theta$  inside the Lyot loop filter. Since each of the passband generated from the Lyot loop filter can be independently

TABLE I  
SEVEN PASSBANDS OF THE MZI-LYOT FILTER BASED MWP MULTIBAND FILTER

Number	Optical comb combination	Tap frequency spacing ( $\Delta\omega$ , pm)	Passband frequency ( $\Omega_b$ , GHz)
#1	Lyot 1	304.2	1.35
#2	Lyot 2	152.1	2.70
#3	MZI - Lyot 2	101.4	4.05
#4	MZI - Lyot 1	76.0	5.40
#5	MZI	60.9	6.75
#6	MZI + Lyot 1	50.8	8.10
#7	MZI + Lyot 2	43.5	9.45

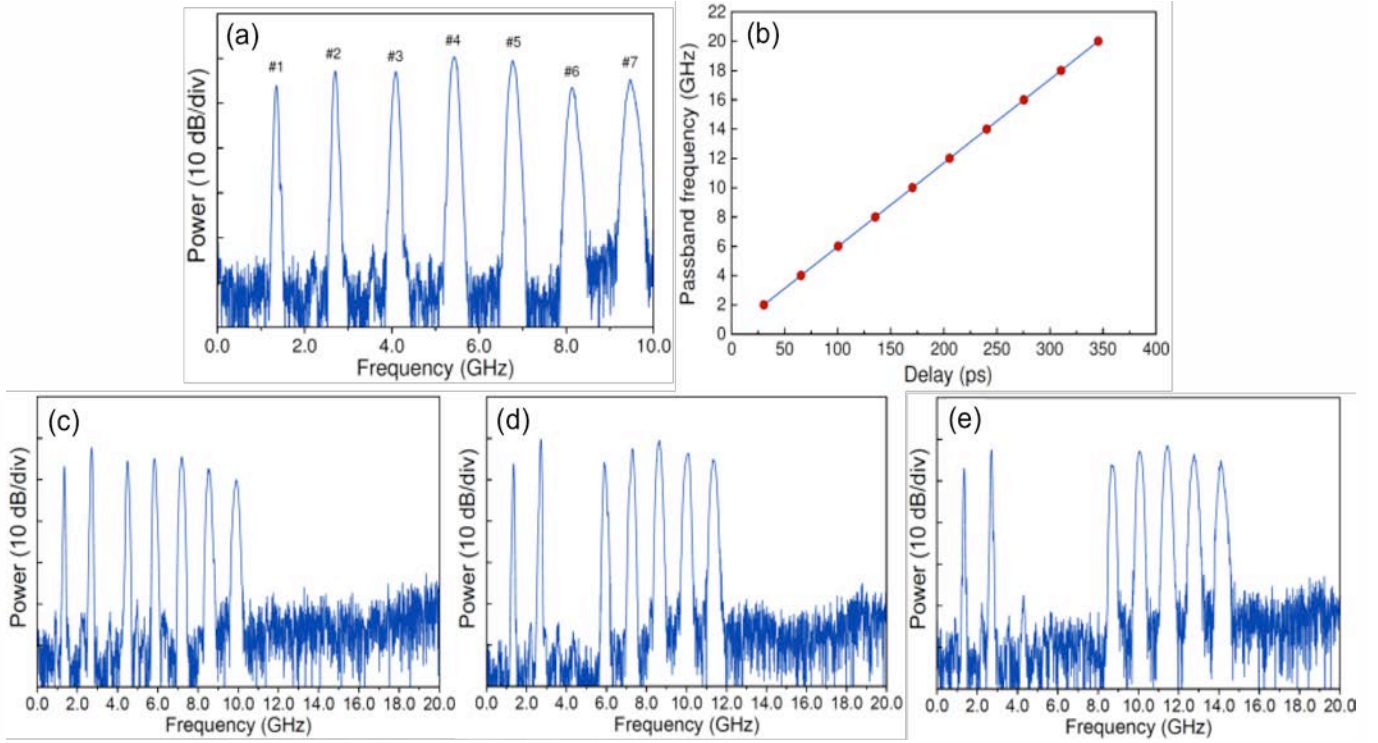


Fig. 4. Demonstration of the continuous tunability of the RF multiband filter. Measure frequency response of the multiband filter. (a) Seven single passbands are evenly distributed from 1.35 GHz to 9.45 GHz, with the same frequency separation of 1.35 GHz between each adjacent passband. (b) Passband frequency tuning in response to the time delay between the two branches of the MZI. (c)-(e) The right five passbands are continuously tuned within a frequency range of 20 GHz.

switched ON or OFF, any passbands generated from Lyot 1 and Lyot 2 are also reconfigurable. From Table 1, one can see that all the passbands except #5 are related to the Lyot loop filter and, therefore, they are all ON/OFF switchable. While passband #5 is also switchable itself through the control of the tunable optical coupler. Furthermore, since the right five passbands (#3 to #7) are continuously tunable, these passbands can be tuned to the frequencies such that they are overlapping with passbands #1 or #2 --- two passbands at the same frequency, acting like one single passband. Figure 5 shows the reconfigured RF multiband filter with different numbers of simultaneous passbands.

Fig. 5(a) to 5(d) are achieved by tuning the right five passbands (#3 to #7) to the same frequencies as the Lyot 1 and Lyot 2 (#1 & #2), such that up to three passbands are overlapping at the same frequency, consequently varying the simultaneous numbers of passband. In particular, in Fig. 5(a) passbands #2 & #3 are at the same frequency, while in Fig. 5(b) passbands #1 & #3 and passbands #2 & #4 are both overlapping. The passband overlapping in RF domain is resulted from the same optical comb spacings generated from the cascaded MZI-Lyot filter and the Lyot loop filter itself. Furthermore, the simultaneous numbers of passbands are adjustable by switching off Lyot 1 or Lyot 2, such that a quad-band filter is resulted. By doing this the frequency spacings of the continuously tunable passbands is adjusted between 1.35 GHz and 2.70 GHz, as shown in Fig. 5(e) and 5(f), respectively. Since both the MZI and Lyot loop filter can be switched off separately, the number of simultaneous passbands can be adjusted to any value from zero to seven.

The current passbands selection is based on polarization state adjustment, high-speed tuning of the passbands can be potentially achieved up to gigahertz speed with the use of nonlinear effect [31]. All the passbands show consistent and stable performance with uniform and sharp passband profiles, and the passband qualities are well maintained during both the tuning and reconfiguring processes. It is worth mentioning that the center frequency of the left two passbands (#1 and #2), which are resulted directly from the Lyot loop filter, are not tunable. These two fixed passbands can be used for fixed channels of an application, and the right five passbands are designed for dynamic channels where channel frequencies need to be adjusted over time. Moreover, for a situation that no fixed channels are needed, the two fixed passbands can be moved to any unused frequencies by adjusting the length of the PMF in the Lyot loop filter to avoid unwanted interferences. Furthermore, the maximum simultaneous passband number can be further increased by using a two-stage cascaded Lyot loop filter [30], or cascading multiple optical interferometric filters to generate more interleaving optical comb [34, 35]. The upper limit is determined by the achievable narrowest passband bandwidth such that all the passbands can fit into the frequency range of interest without interference. Meanwhile, serial and parallel cascading combinations can further increase operation flexibility and reconfigurability, while photonic integration techniques can be used for reducing system complexity and cost [39,40].

Another factor that determines passband center frequencies, bandwidths and frequency spacings of the proposed multiband filter is the amount of dispersion, as shown in Eq. (3) and Eq. (4). Figure 6 shows the above tuning

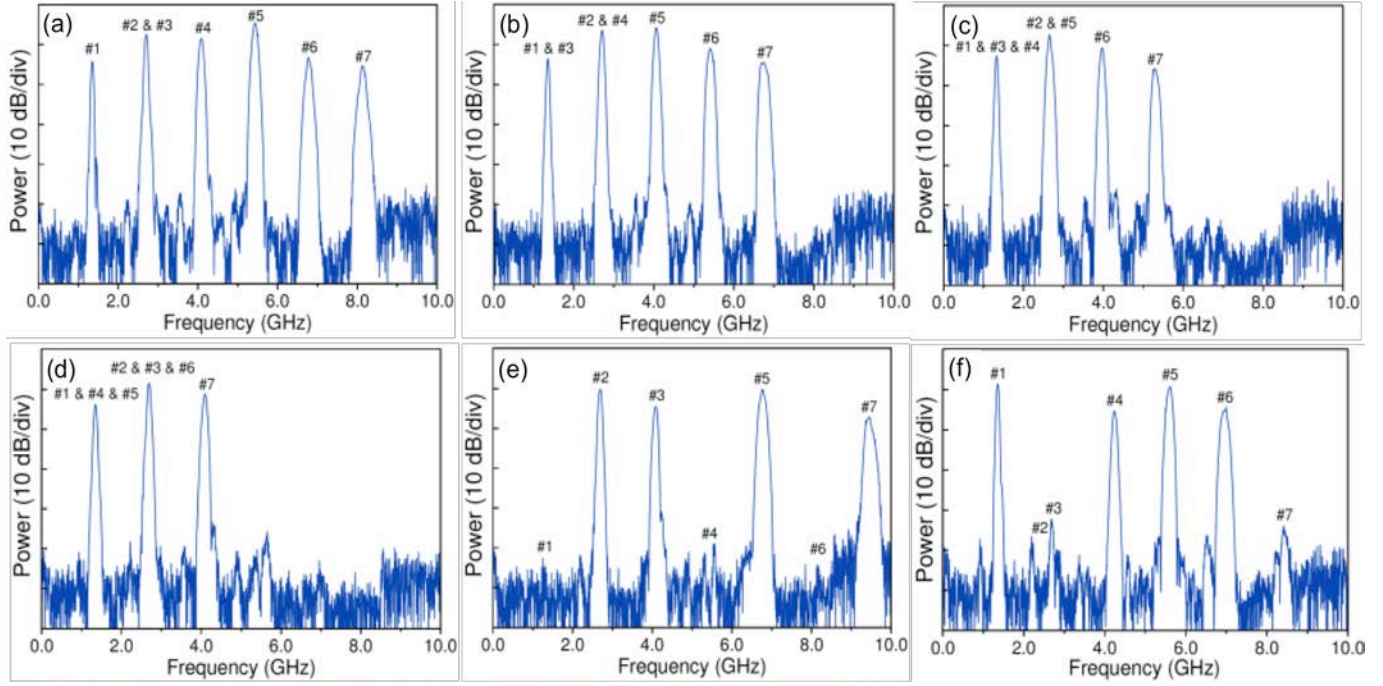


Fig. 5. Demonstration of the passband reconfigurability of the multiband RF filter. The simultaneous passband number is adjusted from three to seven, with different frequency combinations. (a) Six passbands at 1.35 GHz, 2.70 GHz, 4.05 GHz, 5.40 GHz, 6.75 GHz and 8.10 GHz. (b) Five passbands at 1.35 GHz, 2.70 GHz, 4.05 GHz, 5.40 GHz and 6.75 GHz. (c) Four passbands at 1.35 GHz, 2.70 GHz, 4.05 GHz and 5.40 GHz. (d) Three passbands at 1.35 GHz, 2.70 GHz and 4.05 GHz. (e) Four passbands when Lyot 1 (@1.35 GHz) is switched off. (f) Four passbands when Lyot 2 (@2.70 GHz) is switched off.

performance of the multiband filter while the length of the DCF is changed, where the orange filter profiles are captured when a piece of 10.2-km DCF is used and the blue ones are based on a piece of 6.1-km DCF. As shown in Fig. 6(a), with the same MZI and Lyot loop filter, the seven evenly distributed passbands are spread out to a 14 GHz range instead, and the frequency spacing between two adjacent passbands is increased to 1.9 GHz. The average 3-dB bandwidth of the passbands is adjusted from 100 MHz (orange) to 180 MHz (blue). With the same DCF length as in Fig. 6(a), Fig. 6(b) shows the corresponding result when the right five passbands are continuously tuned through temporal adjustment in the MZI. The adjustment of the dispersion and length of PMF of the system is to match the initial design requirements of various applications, and the proposed filter tunability and reconfigurability are not relying on any physical change of the components.

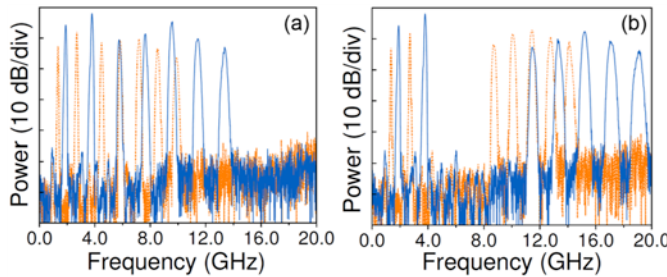


Fig. 6. Passband bandwidth adjustment of the multiband RF filter. The bandwidths of the passbands are broadened with the use of shorter dispersion compensating fiber. Orange: with the use of a piece of 10.2-km DCF; Blue: with the use of a piece of 6.1-km DCF.

#### IV. DISCUSSION AND CONCLUSION

With the fast development of photonic integration techniques, several microwave photonic systems have been successfully integrated as a chip scale device [13,22, 24,36-40]. On-chip optical interferometric filters have been experimentally demonstrated, thus, it is very promising to integrate multiple MZI stages (i.e. core of the proposed reconfigurable multiband filter) into a chip using 2-dimentional mesh structure [39,40]. Since the discrete optical components take most of the space and contribute to most of the loss in the proposed system, we would like to ultimately integrate most of the components on a single chip to reduce the system complexity, SWaP, and cost, while improving overall performance at the same time.

In summary, a photonics based continuously frequency tunable and highly reconfigurable RF multiband filter is proposed and experimentally demonstrated. The number of simultaneous passbands is adjustable from zero to seven, functioning as an all-block, single-band, dual-band, or multiband filter, while the passband frequencies are continuously tunable over 20 GHz range. The scheme utilizes a cascaded MZI and Lyot loop filter architecture, such that various optical comb spacing combinations are obtained for the implementation of the MWP multiband filter. The MSSR of all the passbands are over 35 dB with sharp and uniform passband profiles, providing good filter selectivity. The MWP multiband filter shows stable and consistent performance during the tuning and reconfiguring processes. Furthermore, the proposed work demonstrated a general methodology to implement MWP multiband filters through cascading multiple optical comb filters with various functionalities. In principle,

the proposed multiband filter can potentially support an operation bandwidth up to tens of gigahertz, enabling its applications in 5G networks and ultra-wide broadband systems. Compared to the state-of-the-art RF multiband filters [4], this design significantly increases the simultaneous number of passband as well as providing exceptional broadband operation flexibility, which is the first demonstration of a RF filter with such multiband dynamic capability. The proposed multiband RF filter could significantly enhance the capabilities, functionality, and performance of broadband RF systems. Due to the filter's capability to dynamically tune and reconfigure its passband, the filter can be used for multiband communications in 5G network, radar systems, and RF signal processing applications, where the channel frequencies may need to be dynamically adapted to diverse environments with heterogeneous functions and dynamic spectral availability.

## References

- [1] G. Hueber and R. B. Staszewski, "Multi-mode/Multi-band RF transceivers for wireless communications: Advanced techniques, Architectures, and Trends," John Wiley & Sons, Feb. 2011.
- [2] A. F. Molisch, "Wireless communications," John Wiley & Sons, Sep. 2007.
- [3] J. P. Yao, "Photonics to the Rescue: A Fresh Look at Microwave Photonic Filters," *IEEE Microw. Mag.*, vol. 16, no. 8, pp. 46-60, Sep. 2015.
- [4] R. Gómez-García and A.C. Guyette, "Reconfigurable multi-band microwave filters," *IEEE Trans. Microw. Theory Techn.*, vol. 63, no. 4, pp. 1294-1307, Apr. 2015.
- [5] Y. C. Lin, T. S. Horng, and H. H. Huang, "Synthesizing a Multiband LTCC Bandpass Filter With Specified Transmission-and Reflection-Zero Frequencies," *IEEE Trans. Microw. Theory Techn.*, vol. 62, no. 12, pp. 3351-3361, Dec. 2014.
- [6] K. W. Hsu, J. H. Lin, and W. H. Tu, "Compact sext-band bandpass filter with sharp rejection response," *IEEE Microw. Compon. Lett.*, vol. 9, no. 24, pp. 593-595, Sep. 2014.
- [7] A. C. Guyette, "Intrinsically switched varactor-tuned filters and filter banks," *IEEE Trans. Microw. Theory Techn.*, vol. 60, pp. 1044-1056, 2012.
- [8] J. Capmany, J. Mora, I. Gasulla, J. Sancho, J. Lloret, and S. Sales, "Microwave photonic signal processing," *J. Lightwave Technol.*, vol. 31, no. 4, pp. 571-586, Feb. 2013.
- [9] J. P. Yao, "Microwave photonics," *J. Lightwave Technol.*, vol. 27, no. 3, pp. 314-335, Feb. 2009.
- [10] L. R. Chen, "Silicon photonics for microwave photonic applications," in *Optical Fiber Communication Conference, Optical Society of America*, p. M2B.4, Mar. 2017.
- [11] X. Xue and A. M. Weiner, "Microwave photonics connected with microresonator frequency combs," *Frontiers of Optoelectronics*, vol. 9, pp. 238-248, 2016.
- [12] J. Capmany and D. Novak, "Microwave photonics combines two worlds," *Nature Photon.*, vol. 1, pp. 319-330, June 2007.
- [13] D. Marpaung, B. Morrison, M. Pagani, R. Pant, D. Choi, B. Luther-Davies, S. J. Madden, and B. J. Eggleton, "Low-power, chip-based stimulated Brillouin scattering microwave photonic filter with ultrahigh selectivity," *Optica*, vol. 2, pp. 76-83, 2015.
- [14] J. Ge, H. Feng, G. Scott, and M. P. Fok, "High-speed tunable microwave photonic notch filter based on phase modulator incorporated Lyot filter," *Opt. Lett.*, vol. 40, no. 1, pp. 48-51, Jan. 2015.
- [15] J. Mora, B. Ortega, A. Díez, J. L. Cruz, M. V. Andrés, J. Capmany, and D. Pastor, "Photonic microwave tunable single-bandpass filter based on a Mach-Zehnder interferometer," *J. Lightwave Technol.*, vol. 24, no. 7, pp. 2500-2509, Jul. 2006.
- [16] E. Hamidi, D. E. Leaird, and A. M. Weiner, "Tunable programmable microwave photonic filters based on an optical frequency comb," *IEEE Trans. Microw. Theory Techn.*, vol. 58, no. 11, pp. 3269-3278, Nov. 2010.
- [17] J. Mora, L. R. Chen, and J. Capmany, "Single-bandpass microwave photonic filter with tuning and reconfiguration capabilities," *J. Lightwave Technol.*, vol. 26, no. 15, pp. 2663-2670, Aug. 2008.
- [18] M. Song, C. M. Long, R. Wu, D. Seo, D. E. Leaird, and A. M. Weiner, "Reconfigurable and tunable flat-top microwave photonic filters utilizing optical frequency combs," *IEEE Photon. Technol. Lett.*, vol. 23, pp. 1618-1620, 2011.
- [19] J. Ge and M. P. Fok, "Ultra High-Speed Radio Frequency Switch Based on Photonics," *Sci. Rep.*, vol. 5, no. 17263, pp. 1-7, Nov. 2015.
- [20] X. Xue, X. Zheng, H. Zhang, and B. Zhou, "Tunable chirped microwave photonic filter employing a dispersive Mach-Zehnder structure," *Opt. Lett.*, vol. 36, pp. 3518-3520, 2011.
- [21] X. Xue, Y. Xuan, H. Kim, J. Wang, D. E. Leaird, M. Qi, and A. M. Weiner, "Programmable single-bandpass photonic RF filter based on Kerr comb from a microring," *J. Lightwave Technol.*, vol. 32, pp. 3557-3565, 2014.
- [22] A. Choudhary, I. Aryanfar, S. Shahnia, B. Morrison, K. Vu, S. Madden, B. Luther-Davies, D. Marpaung, and B. J. Eggleton, "Tailoring of the Brillouin gain for on-chip widely tunable and reconfigurable broadband microwave photonic filters," *Opt. Lett.*, vol. 41, no. 3, pp. 436-439, Feb. 2016.
- [23] R. Supradeepa, C. M. Long, R. Wu, F. Ferdous, E. Hamidi, D. E. Leaird, and A. M. Weiner, "Comb-based radiofrequency photonic filters with rapid tunability and high selectivity," *Nature Photon.*, vol. 6, pp. 186-194, Feb. 2012.
- [24] J. Sancho, J. Bourderionnet, J. Lloret, S. Combrié, I. Gasulla, S. Xavier, S. Sales, P. Colman, G. Lehoucq, D. Dolfi, and J. Capmany, "Integrable microwave filter based on a photonic crystal delay line," *Nat. Commun.*, vol. 3, p. 1075, 2012.
- [25] Y. Jiang, P. P. Shum, P. Zu, J. Zhou, G. Bai, J. Xu, Z. Zhou, H. Li, and S. Wang, "A selectable multiband bandpass microwave photonic filter," *IEEE Photon. J.*, vol. 5, no. 3, 5500509, pp. 1-10, June 2013.
- [26] L. Gao, J. Zhang, X. Chen, and J. P. Yao, "Microwave photonic filter with two independently tunable passbands using a phase modulator and an equivalent phase-shifted fiber Bragg grating," *IEEE Trans. Microw. Theory Techn.*, vol. 62, no. 2, pp. 380-387, Feb. 2014.
- [27] J. Ge and M. P. Fok, "Frequency band selectable microwave photonic multiband bandpass filter based on Lyot filter," In *CLEO: Science and Innovations, Optical Society of America*, p. STh3F-2, San Jose, CA, May 2015.
- [28] H. Chen, Z. Xu, H. Fu, S. Zhang, C. Wu, H. Wu, H. Xu, and Z. Cai, "Switchable and tunable microwave frequency multiplication based on a dual-passband microwave photonic filter," *Opt. Express*, vol. 23, no. 8, pp. 9835-9843, 2015.
- [29] L. Huang, D. Chen, F. Zhang, P. Xiang, T. Zhang, P. Wang, L. Lu, T. Pu, and X. Chen, "Microwave photonic filter with multiple independently tunable passbands based on a broadband optical source," *Opt. Express*, vol. 23, no. 20, pp. 25539-25552, Sep. 2015.
- [30] J. Ge and M. P. Fok, "Passband switchable microwave photonic multiband filter," *Sci. Rep.*, vol. 5, no. 15882, pp. 1-8, Nov. 2015.
- [31] J. Ge and M. P. Fok, "Optically Controlled Fast Reconfigurable Microwave Photonic Dual-Band Filter Based on Nonlinear Polarization Rotation," *IEEE Trans. Microw. Theory Techn.*, vol. 65, no. 1, pp. 253-259, Jan. 2016.
- [32] H. Shahoei, M. Li and J. Yao, "Continuously tunable time delay using an optically pumped linear chirped fiber Bragg grating," *J. Lightwave Technol.*, vol. 29, no. 10, pp. 1465-1472, May 2011.
- [33] J. Mora, A. Ortigosa-Blanch, D. Pastor, and J. Capmany, "Tunable microwave photonic filter free from baseband and carrier suppression effect not requiring single sideband modulation using a Mach-Zehnder configuration," *Opt. Express*, vol. 14, no. 17, pp. 7960-7965, July 2006.
- [34] M. P. Fok, and J. Ge, "Tunable Multiband Microwave Photonic Filters," *Photonics*, vol. 4, no. 4, p. 45, Nov. 2017.
- [35] J. Ge, and M. P. Fok, "Continuously tunable and reconfigurable microwave photonic multiband filter based on cascaded MZIs," In *IEEE Photonics Conference (IPC)*, pp. 381-382, Orlando, FL, Oct 2017.
- [36] D. Marpaung, C. Roeloffzen, R. Heideman, A. Leinse, S. Sales, and J. Capmany, "Integrated microwave photonics," *Laser & Photonics Reviews*, vol. 7, no. 4, pp. 506-538, Nov. 2012.
- [37] B. Guan, S. S. Djordjevic, N. K. Fontaine, L. Zhou, S. Ibrahim, R. P.

Scott, D. J. Geisler, Z. Ding, and S.J.B. Yoo, "CMOS Compatible Reconfigurable Silicon Photonic Lattice Filters Using Cascaded Unit Cells for RF-Photonic Processing," *IEEE J. Sel. Topics Quantum Electron.*, vol. 20, no. 4, pp. 359-368, July 2014.

[38] J. S. Fandino, P. Munoz, D. Domenech, and J. Capmany, "A monolithic integrated photonic microwave filter," *Nature Photon.*, vol. 11, pp. 124-129, Dec. 2016.

[39] D. Pérez, I. Gasulla, L. Crudginton, D. J. Thomson, A. Z. Khokhar, K. Li, W. Cao, G. Z. Mashanovich, and J. Capmany, "Multipurpose silicon photonics signal processor core," *Nature communications*, vol. 8, no. 1, p. 636, Sep. 2017.

[40] L. Zhuang, C. G. H. Roeloffzen, M. Hoekman, K. Boller, and A. J. Lowery, "Programmable photonic signal processor chip for radiofrequency applications," *Optica*, vol. 2, no.10, pp. 854-859, Oct. 2015.



**Jia Ge** (S'15) received the B. Eng. degree in electrical engineering from Shandong University, Shandong, China in 2010, and M. Eng. degree in optical engineering from Jinan University, Guangzhou, China in 2013. He is currently working towards his Ph. D. degree in engineering with the Lightwave and Microwave Photonics Lab at the University of Georgia, Athens, GA, USA. His research interests include microwave photonics, fiber optics, optical signal processing, optical communications and optical fiber sensors. He is currently developing photonics based high-speed and dynamic signal processing techniques for broadband RF systems.

Mr. Ge has published over 30 journal and conference papers, and received multiple awards for his research efforts. He is the recipient of 2017 Chinese Government Award for Outstanding Self-Financed Students Abroad, and Brahm P. Verma Award for Academic and Leadership Excellence. Mr. Ge has also received the Dissertation Completion Award and Innovative and Interdisciplinary Research Grant from the University of Georgia.



**Mable P. Fok** (S'02–M'08) received the B.Eng., M.Phil., and Ph.D. degrees in electronic engineering from the Chinese University of Hong Kong (CUHK), Hong Kong, in 2002, 2004, and 2007, respectively. She was a Visiting Researcher at the University of California, Los Angeles (UCLA), CA, USA, and the University of California, Santa Barbara (UCSB), CA, USA, during 2005 and 2006, respectively, where she was engaged in research on supercontinuum generation in nonlinear fibers with the former and all-optical processing of advanced modulation format signals with the latter. After graduation, Dr. Fok joined the Department of Electrical Engineering at Princeton University, Princeton, NJ, USA, as an Associate Research Scholar in 2007, where she was focusing on hybrid analog/digital processing of optical signals based on neuromorphic algorithm and developing new techniques to enhance physical layer information security in optical communications network.

She is currently an Associate Professor and a Distinguished Faculty Fellow in the College of Engineering at

the University of Georgia, Athens, GA, USA. She has published over 170 journal and conference papers. Her recent research interest is on photonic implementation of neuromorphic algorithm and developing new photonic techniques for dynamic and flexible RF communication systems.

Dr. Fok is the recipient of the 2017 NSF CAREER award, 2016 University of Georgia CURO Research Mentoring Award, 2015 University of Georgia College of Engineering Excellence in Research Faculty Award, 2014 Ralph E. Powe Junior Faculty Enhancement Award from ORAU, and 2010 IEEE Photonics Society Graduate Student Fellowship.